


## RESEARCH ARTICLE

WILEY

# Archaeological site formation processes in northwestern Patagonia, Mendoza Province, Argentina

Alfonsina Tripaldi<sup>1,2</sup>  | Marcelo A. Zárate<sup>3</sup> | Gustavo A. Neme<sup>4</sup> | Adolfo F. Gil<sup>4</sup> | Miguel Giardina<sup>4</sup> | M. Laura Salgán<sup>4</sup>

<sup>1</sup>Universidad de Buenos Aires, Facultad de Ciencias Exactas y Naturales, Departamento de Ciencias Geológicas, Buenos Aires, Argentina

<sup>2</sup>CONICET - Universidad de Buenos Aires. Instituto de Geociencias Básicas, Aplicadas y Ambientales de Buenos Aires (IGEBA), Buenos Aires, Argentina

<sup>3</sup>INCITAP-CONICET, Dto. de Ciencias Geológicas, Universidad Nacional de La Pampa, Santa Rosa, La Pampa, Argentina

<sup>4</sup>CONICET- IANIGLA Grupo Vinculado San Rafael/Museo de Historia Natural de San Rafael, UTN Facultad Regional San Rafael, Centro Tecnológico de Desarrollo Regional Los Reyunos, Parque Mariano Moreno, San Rafael, Mendoza, Argentina

## Correspondence

Alfonsina Tripaldi, IGEBA-CONICET, Dto. de Ciencias Geológicas, Universidad de Buenos Aires, Ciudad Universitaria, C1428EHA, Buenos Aires, Argentina.

Email: alfo@gl.fcen.uba.ar

Scientific editing by Cristian Favier Dubois

## Abstract

The Cañadón Amarillo area in northwestern Patagonia (Mendoza Province, Argentina) presents a rich archaeological record contained within thick successions of fine-grained deposits with well-constrained chronological and stratigraphic resolution. Geomorphological, sedimentological, and archaeological analysis of three archaeological localities, constrained by radiocarbon ages, was conducted to reconstruct site formation processes and depositional variability in an exposed, dryland setting. The archaeological sites are located in the Cañadón Amarillo area between the southern margin of the volcanic Payunia Plateau and the Colorado River, in an area of ephemeral streams and eolian sand sheets. The archaeological remains are preferentially contained in fine to very fine sand to silty sand deposits associated with the ephemeral streams. Low-energy fluvial deposition related to overbank flows, and eolian aggradation associated with coppice dunes, sand shadows, and unrippled and partially vegetated mantles have favored preservation of *in situ* archaeological materials. Our investigations provide insight into site formation processes in exposed settings within the semiarid parts of northwestern Patagonia and extend the local record of human occupation to ~7300 <sup>14</sup>C yr B.P.

## KEYWORDS

dryland, fluvial-eolian interaction, hunter-gatherers, Patagonia, site formation processes

## 1 | INTRODUCTION

Most archaeological research in northwestern Patagonia has centered on the analysis of rockshelter sites (Barberena et al., 2011; Borrero, 2004; Durán, 2000; Fernández, 1988–1990) even though ethnoarchaeological studies (Bazzanell & Wierer, 2013; Gorecki, 1988, 1991) and archaeological investigations in other contexts (e.g., Borrero, 1989; Goñi, 1995) demonstrate that rockshelter archaeology by itself is not necessarily representative of past human and ecological systems. Consequently, our understanding of past human dynamics in northwestern Patagonia is biased by the emphasis on rockshelter archaeology. There have been fewer studies of open-air sites and their spatial distribution on the landscape due to an assumption that such sites are young and highly disturbed (Gil & Neme, 2006; Salgán, 2012; Salgán, Gil, & Neme, 2012). In the last decade, however, several open-air sites have been identified and examined, providing new data on past human ecology. These sites have been studied within the geomorphological and sedimentological framework of the landscape, essential for advancing accurate archaeological and paleoecological interpretations (Buck, Kipp, & Monger, 2002; Dincauze, 2000; Schiffer, 1996; Stein & Farrand, 2001).

Here, we report on the geoarchaeological analysis of three open-air archaeological localities in the Cañadón Amarillo area of northwestern Patagonia (Fig. 1). Emphasis is on describing sedimentary depositional variability and evaluating formation processes in a dryland environment that have favored burial and preservation of cultural deposits in good systemic context. The archaeological results are then discussed within a framework of the regional human occupation of northwestern Patagonia. We demonstrate that open-air sites in this part of Patagonia do indeed contain a rich archaeological record extending back to at least the early Holocene.

## 2 | GEOLOGICAL AND ENVIRONMENTAL SETTING

The three archaeological localities, Agua de Pérez, Carmonina, and Colorado Valley, are located in different geomorphic settings within the Cañadón Amarillo area (36°45'S–37°10'S, and 69°14'W–69°30'W) on the southern margin of the Payunia basaltic plateau which rises up to ~1400–1800 m above sea level (asl), ~40 km east of the

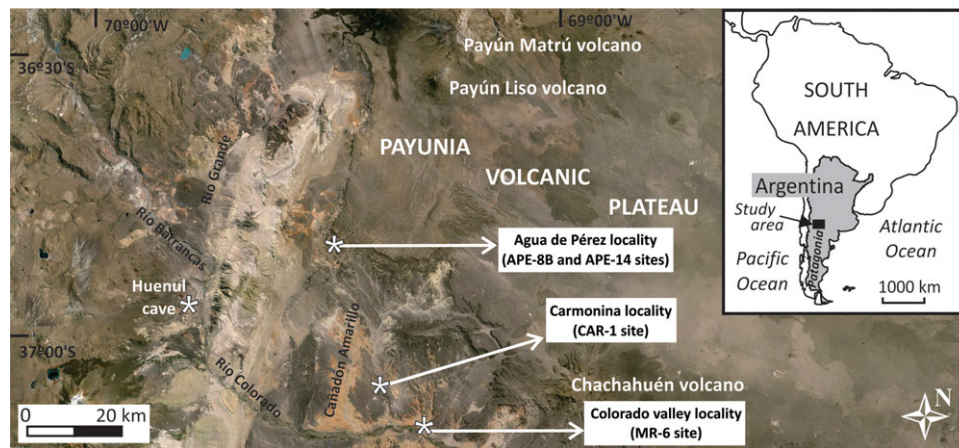


**FIGURE 1** Location of the archaeological localities investigated in the Cañadón Amarillo area, northwestern Patagonia, Mendoza Province, Argentina (satellite image courtesy of Google Earth). Also shown is Huenul Cave, a site of early human occupation located to the west [Color figure can be viewed at [wileyonlinelibrary.com](http://wileyonlinelibrary.com)]

Andes Cordillera (Fig. 1). These localities are situated along ephemeral streams that flow south and join the Colorado River at ~700 m asl. The Payunia plateau consists of extensive lava flows and more than 800 monogenetic basaltic cones with three distinct polygenetic volcanoes, Chachahuén, El Nevado, and Payún Matrú (Llambías, Bertotto, Risso, & Hernando, 2010) that dominate the landscape. Volcanic activity began in the Neogene (26–8 Ma) and continued well into the Holocene (Llambías et al., 2010). Upper Cretaceous sedimentary rocks (epiclastic and calcareous facies), and Neogene sandstones and conglomerates are also exposed in the area (Narciso, Santamaría, Zanettini, & Leanza, 2004).

The Cañadón Amarillo contains a poorly integrated ephemeral fluvial system comprised of discontinuous arroyos fed by mountain winter precipitation and springs on the south slopes of the Payunia plateau. In the study area, the Colorado River channel has a braided pattern (Fig. 2C) developed within an alluvial plain with several reaches entrenched into lava flows of the Payunia Geologic Province (Ramos & Folguera, 2010) and surrounding pediments (Narciso et al., 2004). Desert pavements are common across this region, particularly on the volcanic plateau and pediments.

The study area is part of the South American Arid Diagonal (Bruniard, 1982). Climate is arid to semiarid with mean annual temperature of 14.4°C and average annual precipitation of ~200 mm (Servicio Meteorológico Nacional, 1992). Climatic gradients contribute to an ecotone located between the Monte Desert to the east, influenced by the Atlantic Anticyclone, and the Patagonia Desert to the west, dominated by the action of the Pacific Ocean Anticyclone (Garreaud, Vuille, Compagnucci, & Marengo, 2009).

A Payunia biogeographic district has been recently defined (Martínez Carretero, 2004) with five major plant communities: (a) Patagonian scrub, (b) grasslands of Payunia, (c) Mount Bushes evergreen, (d) psamphilous grassland, and (e) saline soils communities. The dominant soils are poorly developed Entisols, mainly Torripsamments and Torriorthents, with calcic Aridisols on the basaltic plateau (Ferrer & Regairaz, 1993).

### 3 | ARCHAEOLOGICAL OVERVIEW

The archaeological record of northwestern Patagonia is characterized by small- to low-density archaeological sites and scant pottery indicating a hunter-gatherer organizational system. The oldest human occupation in northwestern Patagonia is traced back to ~10,000 <sup>14</sup>C yr B.P. at Huenul Cave (Barberena et al., 2011; Barberena, 2014; Fig. 1). Human evidence from the late Pleistocene is not clear, with no evidence of an association between megafauna and Paleoindian populations (Barberena, 2015; Forasiepi, Martinelli, Gil, Neme, & Cerdeño, 2010; Gil, 2006; Neme & Gil, 2012; Neme et al., 2011).

By ~9000 to 7000 <sup>14</sup>C yr B.P. archaeological evidence becomes more frequent in northwestern Patagonia (Barberena et al., 2010; Barberena, 2014; Berón, 2007; Fernández, 1988–1990; Gil, 2006; Gradín, 1984; Neme et al., 2011), with the exception of Payunia where early Holocene human activity is limited to De Lerma Cave (Gil, 2006). Between 7000–4000 <sup>14</sup>C yr B.P., the regional archaeological record from ~35°S to 39°S latitude is characterized by a broad and significant gap, the origin of which is still debated. Several interpretations have been proposed to explain this hiatus including human depopulation of the area due to increased aridity (Neme & Gil, 2009), extensive volcanic activity (Durán & Mikkan, 2009), and sampling bias (García, 2010).

The regional archaeological record indicates increased occupation after ~4000 <sup>14</sup>C yr B.P., with the abundance of sites and density of cultural material increasing strongly between ~2000 and 1500 <sup>14</sup>C yr B.P. Subsequently, the archaeological record is similar to that of larger northwestern Patagonia (~37–40°S), that is, a hunter-gatherer economy that is quite distinct from the northern “Andean tradition” (~33°–22°S) where agriculture, semi-sedentary villages, and more complex societies are dominant (Lagiglia, 1977, 1980). The driest areas of Payunia were populated during the last ~1500 years (Gil, 2006) where rock shelters and open-air sites show a broad spectrum of foraging activities, with a focus on guanaco hunting. Almost all sites are associated with the few water sources available (mostly temporary), while others are linked to raw material sources (Gil & Neme, 2006).



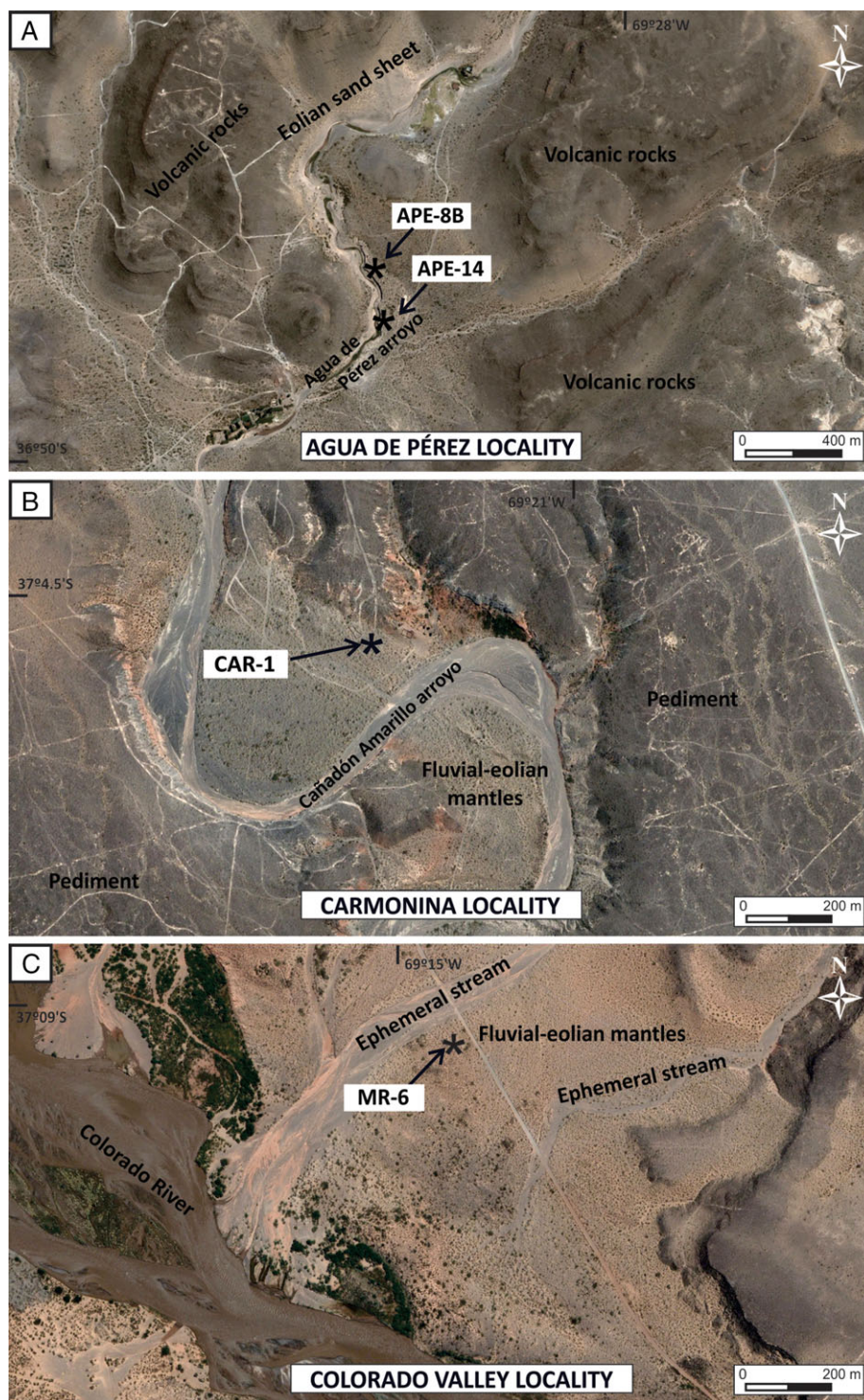


**FIGURE 2** Geomorphic setting of the three study localities. Archaeological sites APE-8B and APE-14 are located in the upper catchment of the Cañadón Amarillo, along the Agua de Pérez arroyo (A). CAR-1 is located in the middle part of the Cañadón Amarillo catchment, inset below a pediment (B). MR-6 is located in the lower part of the Cañadón Amarillo catchment adjacent to the Colorado River (C) [Color figure can be viewed at [wileyonlinelibrary.com](https://onlinelibrary.wiley.com)]

#### 4 | METHODS AND TECHNIQUES

We employed a geoarchaeological approach that included geomorphologic, stratigraphic, and sedimentological analysis at regional, local,

and site scales, together with cultural assemblage studies and radio-carbon dating. Geomorphological analysis involved the use of Landsat satellite imagery, Google Earth® imagery, and digital elevation data (SRTM3), accompanied by field surveys. Archaeological site sediments

**TABLE 1** Radiocarbon dates, reported in conventional and calibrated ages (in years Before Present, yr B.P.), from studied archaeological sites in the Cañadón Amarillo area

Archaeological Site	Unit	Sample	Lab Code	$^{14}\text{C}$ yr B.P.	$\delta^{13}\text{C}$	Cal. yr B.P.*
APE-8B	APE8B A1 N7	Bone	AA-98694	365 $\pm$ 42	−20.1	494 (415) 325
APE-8B	APE8B A1 13 SE	Charcoal	AA-98695	611 $\pm$ 34	−10.4	650 (602) 554
APE-14	Section B	Charcoal	AA-98688	5776 $\pm$ 90	−12.0	6672 (6577) 6470
APE-14	Section A	Charcoal	AA-98687	7340 $\pm$ 120	−21.3	8303 (8160) 8024
CAR-1	S1-Level 6	Charcoal	AA-66576	1398 $\pm$ 39	−21.9	1334 (1312) 1289
CAR-1	A2-Level 11 SW	Charcoal	AA-98684	3589 $\pm$ 28	−21.9	3922 (3892) 3848
CAR-1	A2-Level 17 NE	Charcoal	AA-98685	3980 $\pm$ 28	−22.7	4513 (4471) 4419
CAR-1	A2-Level 21 NE	Charcoal	AA-98686	5661 $\pm$ 47	−21.2	6497 (6443) 6399
CAR-1	A2-Level 23 NE	Charcoal	AA-98689	5516 $\pm$ 42	−20.5	6394 (6315) 6282
MR-6	A1-Level 12 (NO)	Charcoal	AA-98691	607 $\pm$ 34	−11.6	647 (602) 554
MR-6	A1-Level 7 (NO)	Charcoal	AA-98692	754 $\pm$ 34	−24.2	703 (688) 668
MR-6	A1-Level 3 SE	Charcoal	AA-98693	879 $\pm$ 25	−21.4	892 (782) 739
MR-6	A1-Level 19 (NO)	Charcoal	AA-98690	3992 $\pm$ 30	−22.2	4514 (4476) 4423

\*Calibrated and presented at one sigma using OxCal version 4.2 (Bronk Ramsey et al., 2013) and ShCal 13 atmospheric curve (Hogg et al. 2013) using median.

and deposits were described and interpreted following classical facies models (Miall, 1996; Reading, 1996). Stratigraphic sedimentary units were identified according to lithological properties, mainly texture, sedimentary structures, and color (Munsell Color, 2000).

Representative samples were collected from sedimentary units for particle size, carbonate, organic matter (OM), pH, phosphorus, and electric conductivity (CE), analyses performed at INCITAP-CONICET, Universidad Nacional de La Pampa. Samples for particle-size analysis were pretreated to remove organic matter and carbonates, dispersed in an ultrasonic bath and then measured using a Laser Particle Sizer (Malvern 2000). Particle size results were statistically processed and plotted in histograms and cumulative probability frequency curves. Mean and sorting statistical parameters were calculated by the method of moment (Boggs, 2006) and symmetry and kurtosis through graphic formulas after Folk and Ward (1957). General textural characterization of deposits was performed by plotting ratios of sand, silt, and clay in ternary diagrams (Folk, Andrews, & Lewis, 1970). Organic matter contents were determined using the Walkley and Black (1934) method corrected by the 1.72 Van Bemmelen factor; phosphorus contents were determined using the Bray and Kurtz (1945) method. Carbonate contents were quantified with a digital calcimeter (precision of  $\pm 0.1\%$ ).

The archaeological sites were excavated during the 2011 and 2012 field seasons using 10 cm arbitrary levels beginning with Level 1 at the surface. During excavations, the sediment was sieved using a mesh aperture of 2 mm. The sieved samples were separated by flotation in volume of  $\sim 10$  L into light and heavy fractions at the Laboratory of the Natural History Museum of San Rafael (Mendoza, Argentina).

The archaeological deposits were chronologically constrained by 13 accelerator mass spectrometry (AMS)  $^{14}\text{C}$  ages, 12 on charcoal and one from animal bone (Table 1). Ages were calibrated using OxCal version 4.2 (Bronk Ramsey, Scott, & van der Plicht, 2013) based on the ShCal13 atmospheric curve (Hogg et al., 2013)

## 5 | RESULTS

### 5.1 | Agua de Pérez locality

The Agua de Pérez locality is situated in the upper hydrological basin of the Cañadón Amarillo (Fig. 1). The area displays partially dissected, tableland relief with mass wasting deposits along the plateau edge, eolian, and colluvial covers on slopes and edges of ephemeral streams, wet meadows, saline pans, and eolian sand sheets in the lowlands (Fig. 2A). Agua de Pérez is a spring-fed arroyo, characterized by alternating 5 to 20 m deep, entrenched and nonentrenched reaches, typical of discontinuous dryland channels formed in unconsolidated or poorly consolidated deposits (Bull, 1997). Gravel beds interstratified with sandy and silty layers are exposed along the channel walls.

Several archaeological sites were found and studied along the Agua de Pérez arroyo. The two presented here are APE-8B and APE-14, located 250 m apart, along a reach with steep-sided channel walls (Fig. 2A). The APE-8B site ( $36^{\circ}49'31.9''\text{S}$ ,  $69^{\circ}28'43.2''\text{W}$ ) is located at 1573 m asl on a 15 m high terrace (Fig. 3C). Archaeological fieldwork involved the excavation of a 4 m<sup>2</sup> area. Sedimentary deposits at this location are also well exposed along the banks of the Agua de Pérez Arroyo and were described and evaluated (Tripaldi, Zárate, Neme, & Gil, 2015).

The sedimentary succession at APE-8B consists of  $\sim 1.8$  m thick, massive to partially stratified sand and silty sand. The presence of some laminations, bed geometry, and slight differences in color allowed for distinguishing five sedimentary units (Fig. 3 and Table 2). Particle size parameters indicate a general homogenous textural composition with poorly sorted, fine to very fine sands, showing mainly positive asymmetry and leptokurtic to very leptokurtic frequency distributions (Table 3). Moderate bioturbation features (krotovina) formed by roots and faunal burrowing are present. Carbonate nodules (medium sand to granule size) and fine (mm scale) filaments are also common. The ripple to horizontally laminated silty sand of Unit 4 suggests sedimentation



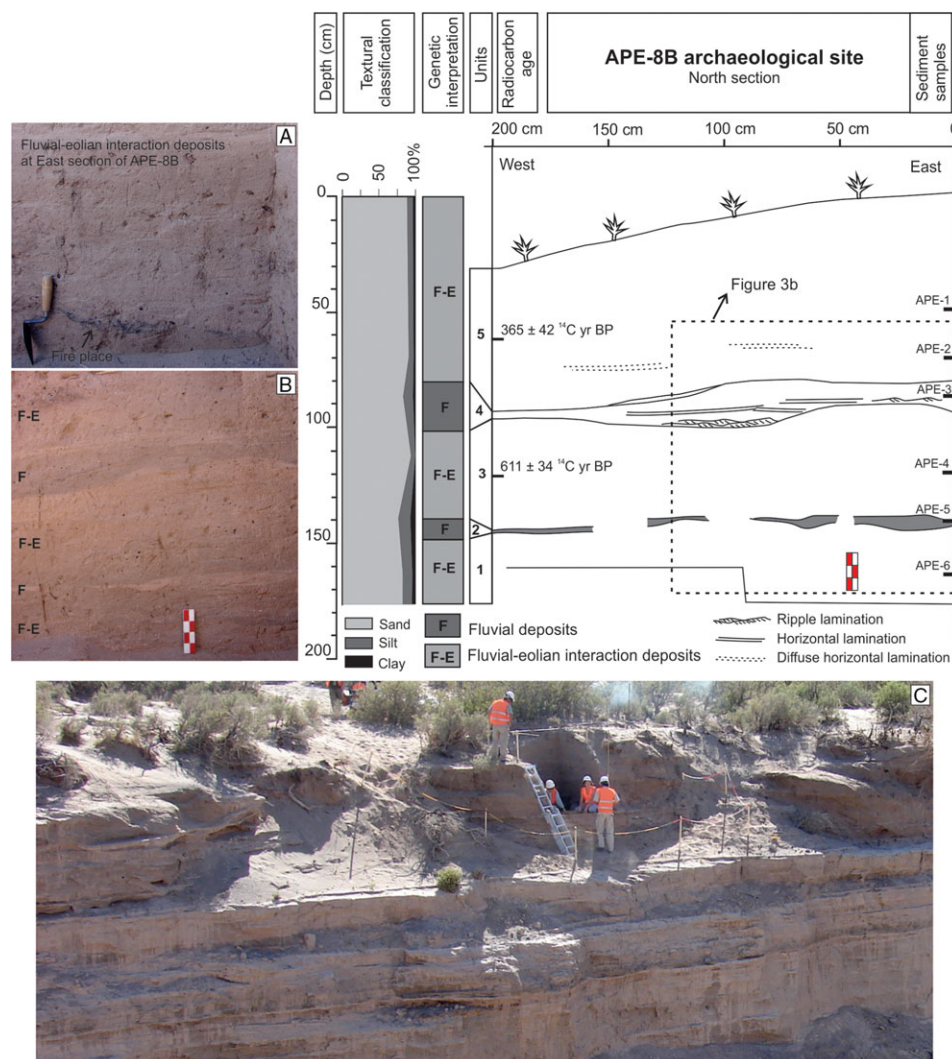


**FIGURE 3** Stratigraphy of the APE-8B site (Agua de Pérez Locality) with particle size distribution, sample locations,  $^{14}\text{C}$  ages, sediment units, and genetic interpretations. Depth (in cm) is from the present surface. Field pictures include (A) deposits in the east section with a hearth at the base, (B) segment of the north section represented in the section drawing (dotted square), and (C) APE-8B location on top of the sedimentary succession at the Agua de Pérez arroyo [Color figure can be viewed at [wileyonlinelibrary.com](http://wileyonlinelibrary.com)]

by low-energy water currents. In Unit 2, relatively high amounts of silt (16.5%) and clay (7.2%) denote accumulation during the final stages of a waning flow, likely out of suspension. The massive silty sands (Units 1, 3, and 5) can be interpreted as the product of flows with high sediment concentrations that preclude the migration of bedforms and function as sandy sediment gravity flows (Miall, 1996), or due to wind sedimentation on partially vegetated surfaces. The dominance of very fine to medium sand (75–85%), absence of granules or pebbles, and low amount of clay (<5%) in these beds, suggest an eolian imprint, either by direct wind deposition or due to the fluvial reworking of eolian deposits (Langford, 1989). This reworking by eolian and fluvial action is also revealed in the similar sand-silt-clay ratio of the fluvial and eolian beds (Fig. 4).

These deposits lack distinct internal bedding, a common feature of eolian sand sheets and fluvial-eolian deposits (e.g., Forman, Tripaldi, & Ciccioli, 2014; Lea, 1990; Tripaldi & Limarino, 2008). Moreover, the geomorphic context of the deposits, dominated by eolian sand sheets

with sand shadows and coppice dunes, supports the interpretation of Units 1, 3, and 5 as accumulated by eolian processes in a partially vegetated eolian sand sheet.

Organic matter values at APE-8B vary between 0.27% and 0.70% (Fig. 5) exhibiting a direct relationship with carbonate content that varies between 0.1% and 1.2% ( $r^2 = 0.93$ ; Fig. 6). pH values range 8.0–8.6 and increase toward the surface but in general indicate an overall alkaline environment (Fig. 5). Phosphorous levels vary between 28.3 and 9.8 ppm and tend to increase toward the top in the upper half of the section (Fig. 5). High levels of phosphorous and pH are correlated (Fig. 6). The upper part of Unit 5 has the highest phosphorous and pH levels, which may reflect recent land use focused on pastoral activity. Similar lower values in Unit 3 and the lower part of Unit 5 are associated with archaeological levels at APE-8B. Unit 1 is distinguished by low organic matter, carbonate, and phosphorous content.

The APE-14 site (36°49'38.23"S, 69°28'41.28"W, Fig. 2A) is located at 1570 m asl and contains a 13.3 m tall stratigraphic exposure in

**TABLE 2** Sedimentary features at the Agua de Pérez archaeological sites

Sedimentary unit	Thickness (cm)	Geometry	Texture	Sedimentary Structure	Color	Carbonate Morphology
APE-8B						
1	30	Tabular	Fine to very fine sand to silty sand; S:Si:C = 88:9:3	Massive	Pinkish gray (7.5YR 6/2)	–
2	<7	Lenticular	Silty sand; S:Si:C = 76:17:7	Massive	Pink (7.5YR 8/4)	Disperse (<5%), medium sand to granule size, carbonate nodules and millimeter filaments
3	<55	Tabular	Fine to very fine sand to silty sand; S:Si:C = 94:6:1	Massive	Pinkish gray (7.5YR 6/2) to light brown (7.5YR 6/3)	
4	<20	Lenticular	Silty sand; S:Si:C = 83:14:4	Current ripple lamination at the base, passing upwards to horizontal lamination	Brown (7.5YR 5/2)	
5	<75	Lenticular	Fine to very fine sand to silty sand; S:Si:C = 89:8:3	Mainly massive or with some diffuse horizontal laminations	Brown (7.5YR 5/2)	
APE-14						
1	580	Tabular	Fine sand; S:Si:C = 92:7:1 with three discrete, <20 cm thick, lenses of pebbly sand (<5% of pebbles of <10 cm in diameter)	Massive	Yellowish brown (10YR 5/4)	–
2	200	Lenticular	Granule to fine to medium pebbles (2–16 mm in diameter)	Massive	Dark gray (7.5YR 4/1 to 10YR 4/1)	–
3	250	Lenticular	Coarse to gravelly sand	Massive and planar cross-bedding	Brown (10YR 5/3)	–
4	300	Tabular	Interlayering of silt, sandy silt, and mud with gastropods and root voids	Massive to millimeter-scale horizontal lamination	Light olive brown (2.5Y 5/3)	–

S:Si:C indicates the proportion of sand (S), silt (Si) and clay (C).

a streamcut where we identified four sedimentary units (Fig. 7 and Table 2). Like with Units 1, 3 and 5 of the APE-8B site, Unit 1 at APE-14 is inferred to have a mixed fluvial-eolian origin. The eolian component is related to coppice and shadow dunes that have been incised in places by streamflow as evidenced by centimeter-thick, lenses of gravelly sand. Units 2 and 3 indicate fluvial sedimentation associated with gravel and sandy bars that are covered by wet meadow deposits in Unit 4.

APE-8 and APE-14 are two of several archaeological sites located along the Agua de Pérez arroyo. Cultural materials from APE-8 were obtained within the 4 m<sup>2</sup> excavation area (Fig. 3). At APE-14, excavations were conducted laterally into the base of the streamcut in two rectangular areas (100 × 20 × 10 cm) comprising Sections A and B (Fig. 7). The archaeological record at both sites is characterized by animal bones, charcoal, and lithics contained within the mixed fluvial-eolian facies (Units 3 and 5 in Fig. 5 and Unit 1 in Fig. 7). The faunal assemblage at both sites includes *Lama guanicoe*, small rodents, Dasipodidae bones and Rheidae eggs shells fragments. At the APE-8 site, two archaeological deposits are separated by a hiatus (Levels 8

and 9), stratigraphically coincident with the fluvial deposits of Unit 4 (Figs. 3 and 5).

Two AMS <sup>14</sup>C dates, 611 ± 34 <sup>14</sup>C yr B.P. (AA-98695) on charcoal in Unit 3 (Level 12, 175 cm depth) and 365 ± 42 <sup>14</sup>C yr B.P. (AA-98694) on animal bone in Unit 5 (Level 6, 115 cm depth; Fig. 3 and Table 1) provide a relatively recent chronology for the APE-8B archaeological deposits. In the case of APE-14, two AMS <sup>14</sup>C dates on charcoal yielded ages of 7340 ± 120 <sup>14</sup>C yr B.P. (AA-98687) at Section A, and 5776 ± 90 <sup>14</sup>C yr B.P. (AA-98688) at Section B (Fig. 7 and Table 1).

Discrete archaeological assemblages found along the Agua de Pérez Arroyo indicate multiple, short, human occupations through time within a relatively small area. The assemblages are interpreted as distinct events of short-term hunter-gatherer human occupation, in which different activities took place, mostly associated with animal processing and consumption, stone tool making and probable plant processing. Considering that the Agua de Pérez locality is next to a siliceous raw material source (Salgán et al., 2012) and that the number of flakes and tools recovered from the site is relatively low, it is likely that the main activity at these sites was associated with food procurement.

TABLE 3 Grain-size parameters of sediment samples from the Cañadón Amarillo archaeological sites

Sample	Site (depth)	Unit	Mean	SD	Mode	φ 1%	Median	K <sub>G</sub>	SK <sub>1</sub>	VCS (%)	CS (%)	MS (%)	FS (%)	VFS (%)	Sand (%)	Silt (%)	Clay (%)
APE-01	APE-8B (102 cm)	5	2.8	1.3	2.00–2.50	0.5	2.6	1.8	0.2	0.0	3.8	29.6	38.9	16.0	88.3	8.6	3.1
APE-02	APE-8B (123 cm)	5	2.7	1.2	2.00–2.50	0.6	2.6	1.5	0.2	0.0	4.9	29.4	39.5	16.6	90.4	6.9	2.7
APE-03	APE-8B (140 cm)	4	3.3	1.1	2.00–2.50	1.2	3.0	2.2	0.1	0.0	0.5	13.6	37.9	30.7	82.8	13.7	3.6
APE-04	APE-8B (166 cm)	3	2.5	1.0	2.00–2.50	0.3	2.5	1.2	0.1	0.4	6.9	26.6	39.5	20.2	93.6	6.0	0.5
APE-05	APE-8B (193 cm)	2	3.3	2.2	2.00–2.50	0.0	2.6	1.7	0.5	0.0	9.4	25.2	25.7	15.9	76.2	16.5	7.2
APE-06	APE-8B (217 cm)	1	3.1	1.5	2.00–2.50	0.2	2.9	1.5	0.2	0.0	6.6	21.0	32.1	22.6	82.3	13.2	4.5
APE12-01	APE14 (1220 cm)	1	2.4	1.1	2.00–2.50	0.0	2.5	1.2	0.1	1.4	9.7	27.8	36.0	16.8	91.8	8.1	0.2
APE12-02	APE14 (1165 cm)	1	2.2	1.0	1.50–2.00	0.2	2.1	1.5	0.1	0.5	11.4	38.3	34.2	8.3	92.7	6.2	1.1
CAR-01	CAR-1 (420 cm)	1	2.3	0.7	2.00–2.50	0.6	2.3	1.2	0.0	0.0	3.2	35.6	45.7	12.8	97.4	2.6	0.0
CAR-02	CAR-1 (260 cm)	2	2.2	0.8	2.00–2.50	0.4	2.1	1.0	0.2	0.0	4.5	38.8	44.0	11.1	98.4	1.7	0.0
CAR-03	CAR-1 (206 cm)	4	3.8	1.3	3.50–4.00	0.9	3.6	1.3	0.2	0.0	1.2	8.2	21.5	32.9	63.7	33.8	2.5
CAR-04	CAR-1 (205 cm)	5	3.3	1.1	3.00–3.50	0.8	3.2	1.2	0.1	0.0	1.1	11.3	29.0	34.6	76.0	22.8	1.2
CAR-05	CAR-1 (178 cm)	5	2.7	0.8	2.50–3.00	1.0	2.6	1.1	0.1	0.0	0.8	22.2	46.0	24.6	93.6	6.1	0.3
CAR-06	CAR-1 (160 cm)	5	2.5	0.8	2.00–2.50	0.8	2.5	1.3	0.1	0.0	1.9	29.2	45.4	17.6	94.1	5.5	0.5
CAR-07	CAR-1 (130 cm)	5	2.5	0.8	2.00–2.50	0.8	2.6	0.9	0.0	0.0	1.6	27.7	46.8	19.5	95.6	4.0	0.4
CAR-08	CAR-1 (90 cm)	5	2.5	0.8	2.00–2.50	0.6	2.5	1.0	−0.1	0.0	2.7	30.5	44.8	17.7	95.7	3.8	0.5
CAR-09	CAR-1 (60 cm)	5	2.6	1.0	2.00–2.50	0.6	2.4	1.7	0.2	0.0	3.2	29.9	42.9	17.0	93.0	5.5	1.5
MR6-05	MR-6 (95 cm)	5	2.9	0.9	2.50–3.00	1.2	2.9	1.2	0.2	0.0	0.0	15.6	45.9	29.7	91.2	7.8	1.0
MR6-01	MR-6 (115 cm)	3	2.6	1.5	2.50–3.00 (−0.50 to 0.00)	0.0	3.7	1.6	0.0	14.2	2.1	9.8	35.9	27.4	89.3	9.3	1.4
MR6-02	MR-6 (118 cm)	3	1.3	0.9	1.00–1.50	−0.5	1.3	1.4	0.2	7.5	37.4	38.2	11.1	1.9	96.1	3.5	0.5
MR6-03	MR-6 (123 cm)	4	3.9	1.3	3.50–4.00	1.3	3.8	1.5	0.2	0.0	0.3	5.1	20.3	35.9	61.7	35.4	3.0
MR6-04	MR-6 (162 cm)	3	3.0	0.8	2.50–3.00	1.2	3.0	1.3	0.0	0.0	0.0	13.2	46.1	32.1	91.4	7.4	1.2
MR6-06	MR-6 (190 cm)	3	2.7	0.7	2.50–3.00	1.2	2.6	1.1	0.1	0.0	0.1	22.6	48.3	24.0	95.0	4.5	0.5
MR6-07	MR-6 (128 cm)	3	2.5	0.9	2.50–3.00	0.6	2.6	1.1	0.0	0.0	4.7	28.2	41.1	20.6	94.6	5.0	0.4
MR6-08	MR-6 (291 cm)	2	2.8	0.9	2.50–3.00	0.4	2.3	1.2	0.1	0.0	1.0	22.1	42.4	25.7	91.3	8.2	0.6

References: mean and mode in phi units; SD, standard deviation; K<sub>G</sub>, kurtosis; SK<sub>1</sub>, asymmetry; VCS, very coarse sand; CS, coarse sand; MS, medium sand; FS, fine sand; VFS, very fine sand (according to Udden–Wentworth grain-size scale).

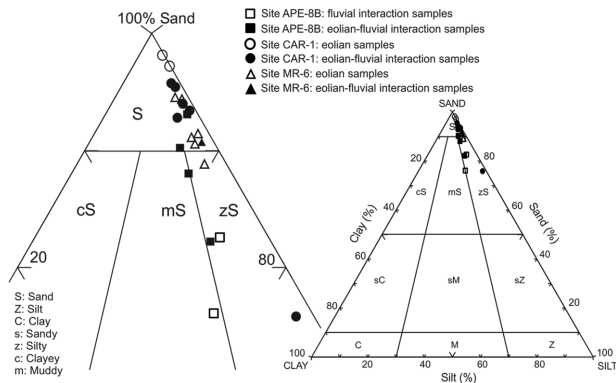


**FIGURE 4** Textural classification of archaeological site sediments (after Folk et al., 1970)

## 5.2 | Carmonina locality

The Carmonina locality is situated within the alluvial plain of the Cañadón Amarillo arroyo where it is inset below a pediment etched into Cretaceous red beds and bordered by a <5 m thick veneer of colluvial gravels and blocks (Figs. 2B and 8F). In this area, the arroyo has a meandering channel, confined within a ~40 m deep and 50 to 600 m wide valley. The channel contains longitudinal bars and lag deposits, dominated by pebbles and cobbles (up to ~1 m in diameter), mainly (~95%) of basaltic composition, and accompanied by poorly sorted, red and yellow, coarse to medium sand. Interchannel areas are characterized by fluvial-eolian deposition with small, sand-bed arroyos, patches of loose fine-very fine sand with coppice dunes and eolian ripples.

The CAR-1 archaeological site (37°04'33.86"S, 69°21'21.46"W; Figs. 1 and 2B) is located at 850 m asl on the inside bend of a large

meander, about 100 m north of the present Cañadón Amarillo main arroyo channel (Fig. 2B). Archaeological fieldwork included an 8 m<sup>2</sup> excavation extending to 2.8 m depth with an additional 1 m<sup>2</sup> test pit extending to 4.2 m depth inside the larger excavated area. CAR-1 deposits are dominated by massive fine sand, with two tephra layers and overlying subordinate lenses of granules and fine pebbles. Five sedimentary units were distinguished (Fig. 8 and Table 4). There are some bioturbation features, mainly rodent krotovina, concentrated within ~10 cm below the tephra layers (Fig. 8C and D).

The textures of Units 1 and 3 at CAR-1 (moderate well sorted, fine sand with traces of silt and no clay and gravel) point to an eolian origin. Similar to some of the sandy beds at APE-8B and APE-14, the massive (non-bedded) nature of these deposits is here interpreted as the product of aggradation in a partially vegetated, eolian sand sheet with localized coppice dunes and sand shadows (Lea, 1990). Units 2 and 4 are tephra layers related to episodic volcanic activity in the Andes to the west (Stern, 2004). The smooth convex to concave geometry of the Unit 4 tephra layer is interpreted as the preservation of the smooth relief of an eolian sand shadow (Fig. 8C). Unit 5 at the surface contains fluvially dominant sediment, accumulated by ephemeral sheet floods with some secondary flood channels resulting in a few pebbly deposits. Eolian deposition cannot be excluded considering the predominance of fine sand and low silt content. These sediments suggest a fluvial-eolian depositional setting, similar to the present Carmonina locality environment.

Organic matter values in Units 1–5 range between 0.26% and 0.06%, and tend to covary with carbonate content that ranges 0.5 – 2.9% ( $r^2 = 0.49$ ; Fig. 6). pH levels range 7.6–8.7 and display a general decrease from top to bottom with some variability in Unit 5 (Fig. 9). Phosphorous values range 2.80–10.96 ppm, and also show a decrease-

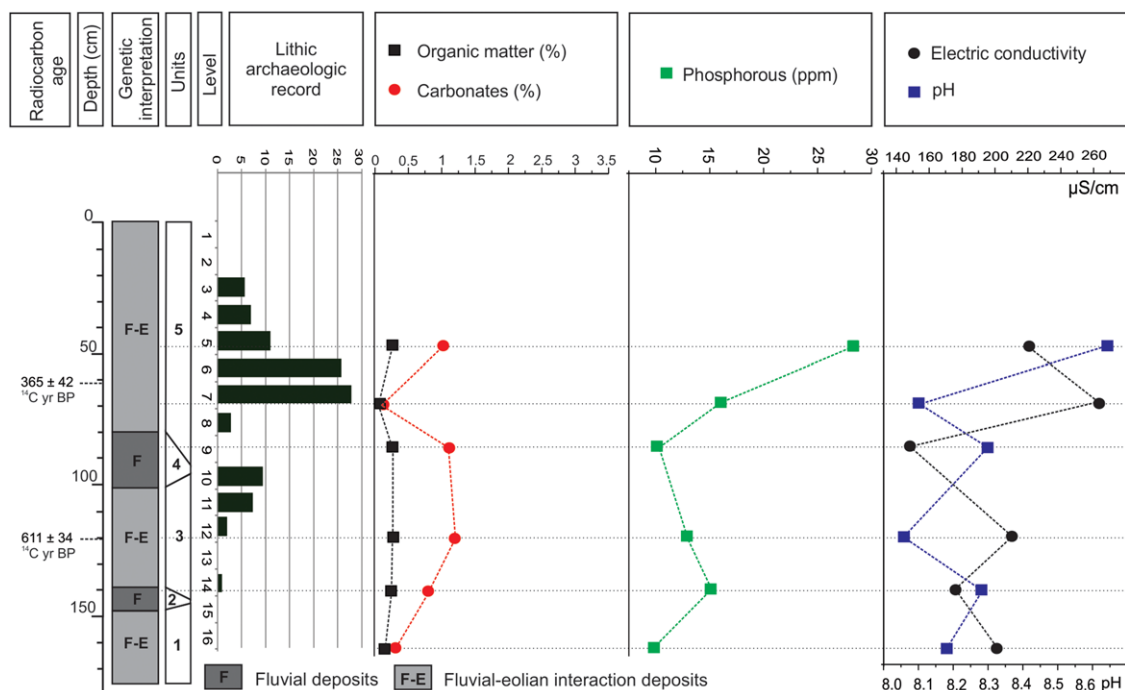


**FIGURE 5** Archaeological lithic material and chemical parameters in relation to sediment units and their genetic interpretations at APE-8B (Agua de Pérez Locality) [Color figure can be viewed at [wileyonlinelibrary.com](http://wileyonlinelibrary.com)]



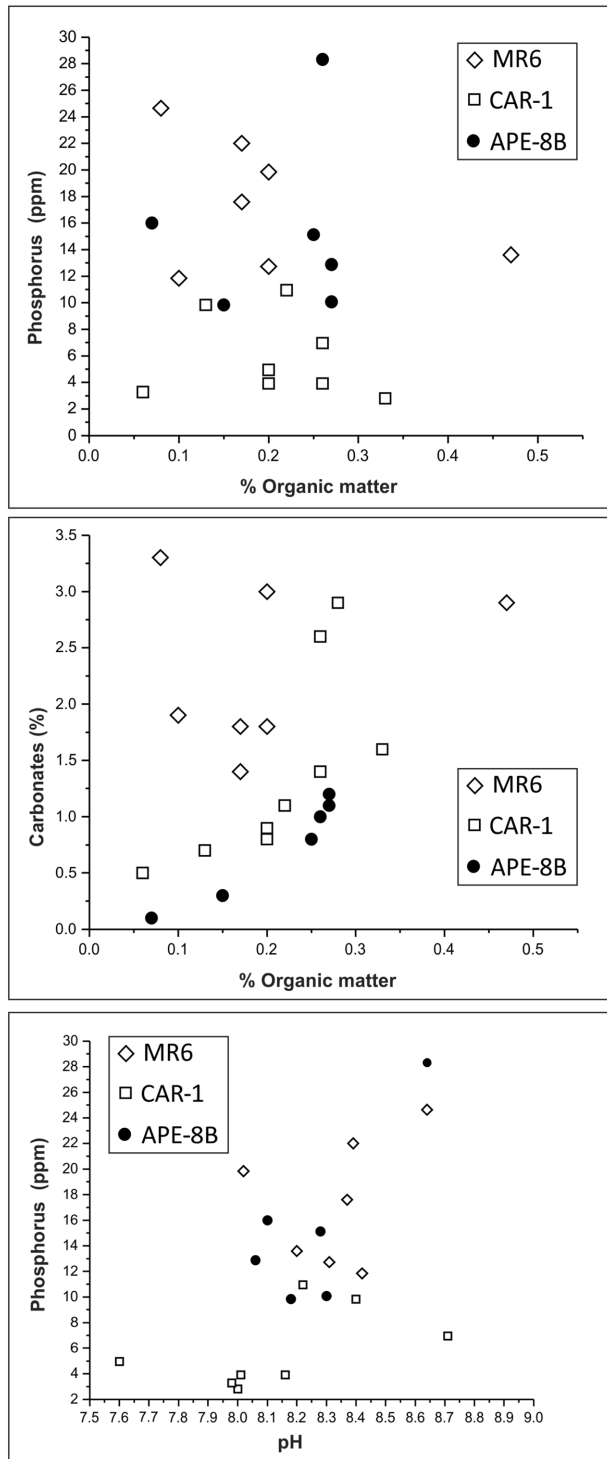


**FIGURE 6** Bivariate plots of phosphorus, carbonate, organic matter, and pH from APE-8B, CAR-1, and MR6

ing trend with depth (Fig. 9). The phosphate value in Unit 5 is higher than in Units 1 to 4. As a result, Unit 5 exhibits a different chemical signature with highest values in organic matter, phosphorous, and pH.

Archaeological materials at CAR-1 were recovered in the upper 2.3 m, that is, in Unit 5 and the upper 30 cm of Unit 3 (Fig. 9). Artifacts are not homogeneously distributed through the sedimentary succession. On the contrary, more than 98% of the artifacts are contained within

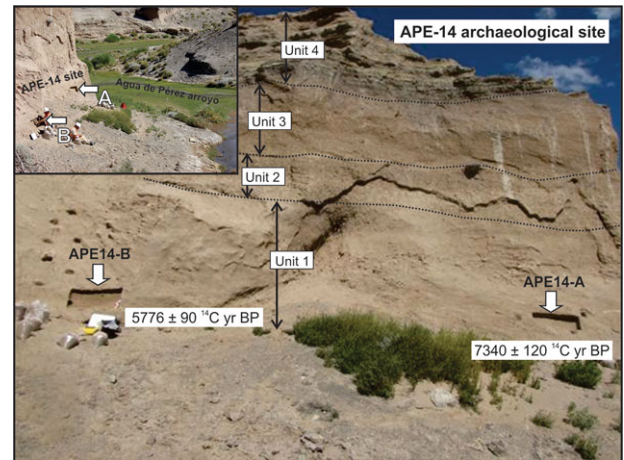


**FIGURE 7** Sedimentary units and bulk sediment sampling in two sections (A and B) at APE-14, placed at the base of a sedimentary succession exposed by the Agua de Pérez arroyo. Radiocarbon ages are on charcoal recovered from sections A and B [Color figure can be viewed at [wileyonlinelibrary.com](http://wileyonlinelibrary.com)]

Unit 5 (Fig. 9). Below this level there is a gap, with smaller concentrations of cultural material at 200–230 cm depth in Unit 3. The cultural assemblage is dominated by lithics (preliminary estimation  $n = 3641$ ) including mostly flakes (predominantly silica-rich volcanics and basalt), stone instruments, and milling stones. Other cultural materials include small amounts of charcoal, egg shells, and bone fragments. The relatively low recovery of organic materials in relation to lithics could be related to local conditions unfavorable for the preservation of organic matter. The archaeological record suggests that knapping and plant and animal processing were the main activities at CAR-1.

Five charcoal AMS <sup>14</sup>C ages from CAR-1 constrain the final sediment accumulation of Units 3 at ~5700–5500 <sup>14</sup>C yr B.P. and Unit 5 between ~4000–1400 <sup>14</sup>C yr B.P. (Figs. 8 and 9; Table 1). The lower ash fall event occurred before ~5700 <sup>14</sup>C yr B.P. and the second between ~5700 and ~4000 <sup>14</sup>C yr B.P. (Fig. 9). The two lowermost charcoal samples are vertically separated by 10 cm and have slightly inverted ages (Fig. 9) but are temporally equivalent within their standard error ranges.

The <sup>14</sup>C chronology confirms episodic human occupation at CAR-1 over the past 5700 <sup>14</sup>C years (Fig. 9 and Table 1). The distribution of archaeological remains suggests an initial low intensity use of the site with higher intensity human occupation over the last ~4000 <sup>14</sup>C years after the second volcanic eruption and tephra layer (Fig. 9).

### 5.3 | Colorado Valley locality

The Colorado Valley locality is situated at the terminal reach of the Cañadón Amarillo fluvial system (Fig. 1). A series of ephemeral streams drain the pediments and edges of the volcanic plateau (Fig. 2C). Interchannel areas are covered by gravely sand in association with eolian sand sheets and partially vegetated, small (<6 m high) coppice dunes with rippled and unrippled beds. The MR-6 Site (37°9'5.67"S, 69°14'52.18"W) is located at 700 m asl, ~700 m north of the present Colorado River channel (Figs. 2C and 10C). An approximately 4 m<sup>2</sup> area

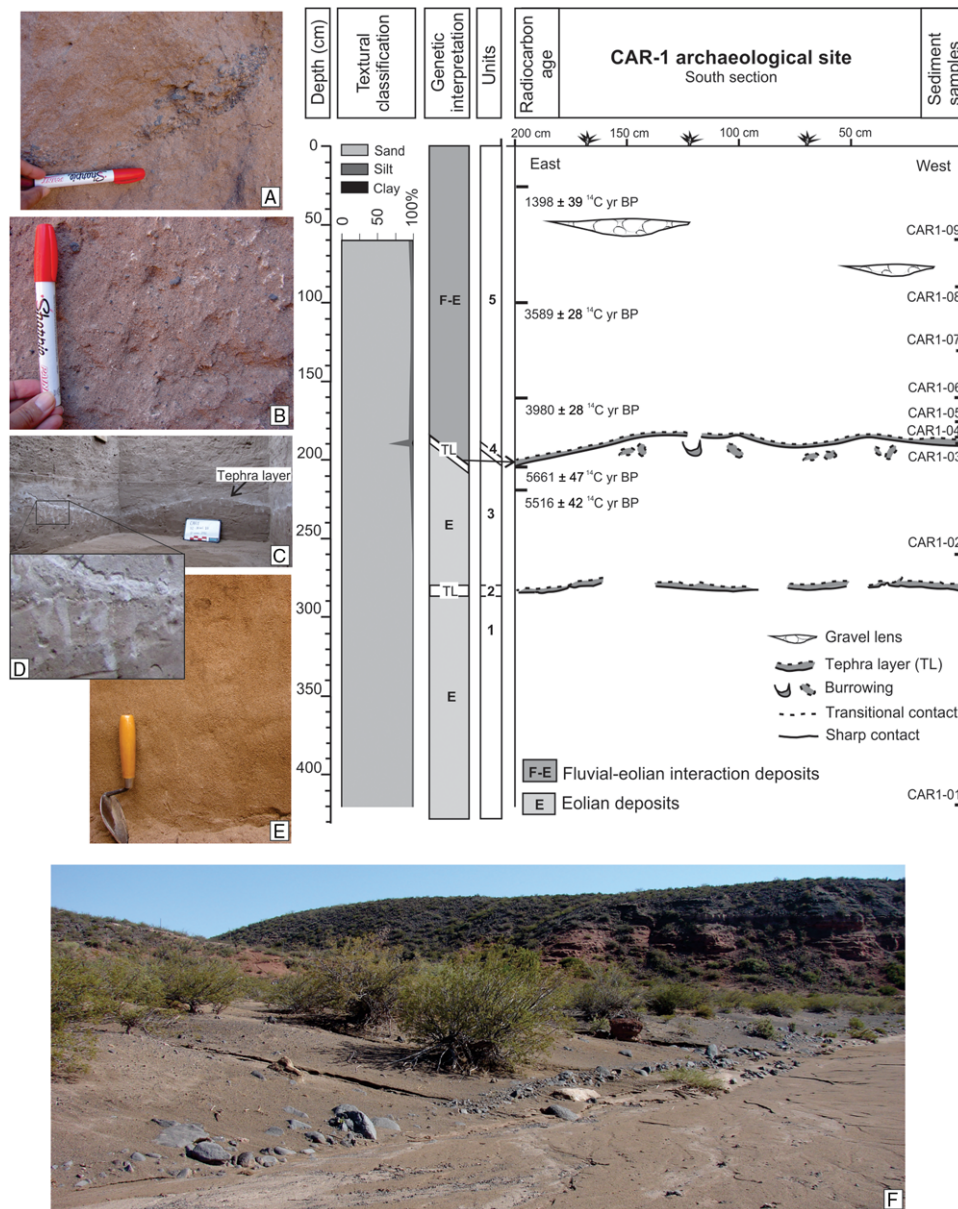


**FIGURE 8** Stratigraphy at CAR-1 (Carmonina locality), with particle size, sample location, <sup>14</sup>C ages, sediment units, and genetic interpretations. Field pictures include (A) detail of one of the pebbly channel deposits within Unit 2, (B) sand with some scattered granules and pebbles of Unit 2, (C) tephra layer overlying the eolian sand of Unit 3, (D) detail of the intense burrowing below the tephra layer, (E) eolian sand within Unit 1, and (F) geomorphic context of the archaeological site with the gravelly sand alluvial plain and outcrops of Cretaceous red beds [Color figure can be viewed at [wileyonlinelibrary.com](http://wileyonlinelibrary.com)]

of the site was excavated to 3.6 m depth into the side of a coppice dune. The site is characterized by more sedimentary variability (boulder to fine sand) compared to APE-8B, APE-14, and CAR-1. Five sedimentary units were identified (Fig. 10 and Table 4) and laterally traceable along the north, east, and south walls of the excavation.

Gravels and boulders within the basal Unit 1 indicate high-energy deposition by traction currents resulting in longitudinal bars or channel lags (Miall, 1996), similar to those presently transported and deposited by arroyos in the lower reach of the Cañadón Amarillo fluvial system (Fig. 2C). Unit 2 is interpreted as the product of lower energy fluvial currents that deposited fine sand with dispersed basalt granules and pebbles. The textural characteristics and current eolian environ-

ment with sand sheets point to some wind sorting of this sediment. This sedimentary unit is comparable to the fluvially reworked eolian sand (fluvial-eolian interaction facies) described by Newell (2001). The reddish (5–7.5 YR) colors are inherited from red sandstones that outcrop to the north (Fig. 1). Finally, the sequence is capped by Units 3 and 5 that contain cross-laminated beds of moderately sorted fine sand and formed by eolian sedimentation associated with the surface dune (Fig. 10C). A single tephra layer occurs at 115–120 cm below the present surface.

Organic matter values range 0.10–0.47% with the highest content near the surface. Carbonate content varies between 1.4% and 3.3% with the highest percentages in Units 2 and 5 (Fig. 11). pH and

**TABLE 4** Sedimentary features at Carmonina (CAR-1) and Colorado Valley (MR-6) localities

Sedimentary Unit	Thickness (cm)	Geometry	Texture	Sedimentary Structure	Munsell Color	Carbonate Morphology
CAR-1 (from base to top)						
1	130	Tabular	Moderately fine sand; S:Si:C = 97:3:0	Massive	Brownish yellow (10YR 6/6)	Few (<5%) millimeters nodules
2 Tephra layer	<2	Discontinuous and irregular	Fine ash	Massive	Very pale brown (10YR 8/2)	Carbonate in the sedimentary matrix
3	190	Tabular transitional	Moderately fine sand; S:Si:C = 98:2:0	Massive	Brownish yellow (10YR 6/6)	Few (<5%) millimeters nodules
4 Tephra layer	2	Tabular, convex-upward bed with ~30 cm in relief	Fine ash; S:Si:C = 64:34:2	Massive	Very pale brown (10YR 8/2)	Carbonate in the sedimentary matrix
5	200	Tabular	Moderately fine sand with disperse, <5% of granules and fine pebbles; S:Si:C = 94:5:1 With few discrete, ~5–10 cm thick lenses of fine pebbles (2–8 mm in diameter)	Massive	Light brown (7.5YR 6/3)	
MR-6 (from base to top)						
1	50	Lenticular	Subangular to subrounded, basalt boulders (40 cm of maximum diameter) in a moderately sorted, sandy matrix.	Massive	Black (5YR 2.5/1)	–
2	<80	Lenticular	Moderately sorted, fine sand with <5% of basalt granules and fine pebbles (2–8 mm in diameter). S:Si:C = 95:5:0	Massive	Yellowish red (5YR 5/6)	Few (<5%) millimeters nodules
3	140	Tabular	Moderately well sorted, fine sand; S:Si:C = 92:7:1.	Cross-bedding, with millimeter-thick foresets dipping 15–28°	Light brown (7.5YR 6/4)	
4 Tephra layer	<3	Discontinuous and irregular	Fine ash; S:Si:C = 62:35:3	Massive	Very pale brown (10YR 8/2)	Carbonate in the sedimentary matrix
5	115	Tabular	Moderately well sorted, fine sand.	Cross-bedding, with millimeter-thick foresets dipping 25°	Light brown (7.5YR 6/4)	

S:Si:C indicates the proportion of sand (S), silt (Si), and clay (C).

phosphorus levels vary 8.0–8.6 and 11.8–24.6 ppm, respectively (Fig. 6). With the exception of increased pH and decreased EC in the tephra layer; there is no clear chemical trend with depth.

The earliest archaeological evidence at MR-6 consists of some flakes and low-density charcoal in Unit 2, just above the basalt boulders (Fig. 11). Above this are three discrete artifact levels within the stratified sands of Unit 3. The lowermost layer is mainly represented by camelid bones, flakes, and one hearth (charcoal concentration), 210 cm below the present surface (Fig. 11). The second level is composed of stone flakes, charcoal, camelid, and medium mammal bones at 155–165 cm below the present surface (Fig. 11). Finally, a

grinding stone was found above the tephra layer (Fig. 10) that was laterally associated (same depth) to fish bones and charcoal remains. Fish bones are notoriously abundant in MR-6 deposits with remains of *Diplomystes* sp. and *Percichthys* sp. in Unit 3 and specimens of *Percichthys* sp. in Unit 2. Corbat (2016) concluded that these ichthyofaunal materials are consistent with the existence of, at least, two taphonomic processes. The oldest assemblage is in Unit 2 and dated to ~4000 <sup>14</sup>C yr B.P. (Fig. 11). This assemblage has low-density and taxonomic diversity with no signs of combustion, which, given the fluvial context, suggest a noncultural origin. The younger assemblage dated to ~600–900 <sup>14</sup>C yr B.P. in Unit 3 has a higher density of



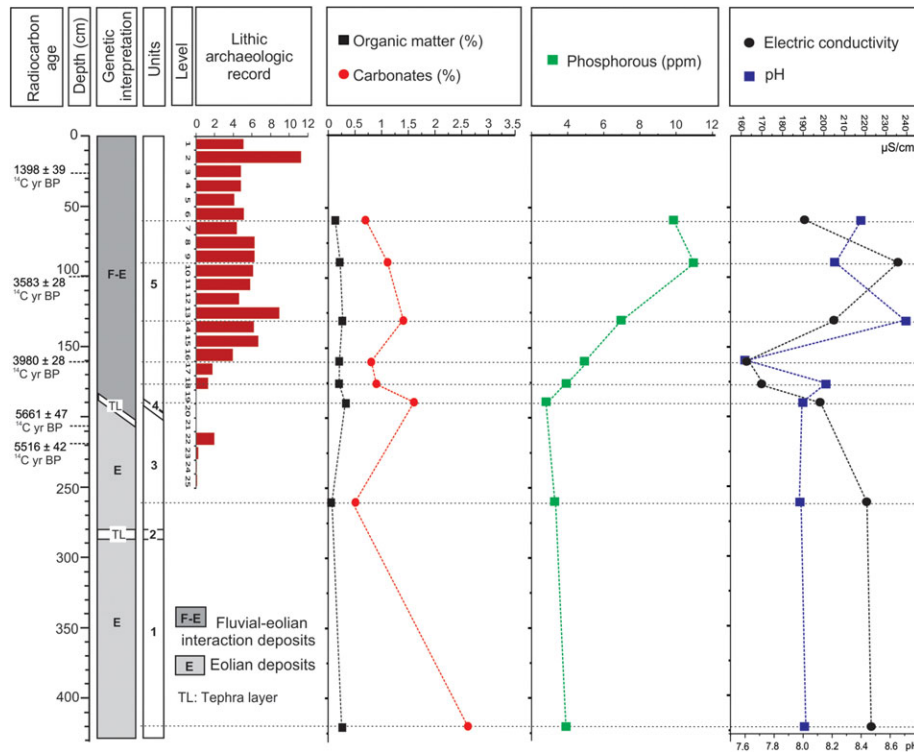


**FIGURE 9** Archaeological lithic material and chemical parameters in relation to sediment units and their genetic interpretations at CAR-1 (Carmonina locality) [Color figure can be viewed at [wileyonlinelibrary.com](http://wileyonlinelibrary.com)]

fish bones, a greater diversity of species, and are thermally altered, suggesting an anthropogenic origin associated with human occupation. That the upper three  $^{14}\text{C}$  ages within Unit 3 are stratigraphically inverted (Figs. 10 and 11; Table 2) is not unusual for eolian contexts (Buck et al., 2002). We consider the archaeological remains within Unit 3 to represent periodic human occupation between  $\sim 600\text{--}900$   $^{14}\text{C}$  yr B.P.

## 6 | DISCUSSION

### 6.1 | Site formation processes and the archaeological record

Most archaeological studies in northwestern Patagonia have taken place in rockshelters (Barberena et al., 2011; Borrero, 2004; Durán, 2000; Fernández, 1988–1990; Gil, 2006) ostensibly under the assumption that open-air sites in this area do not have a buried archaeological record with a deep chronology of human occupation, despite some evidence to the contrary (e.g., Gradín, 1986). Our investigation presents three archaeological sites with thick sedimentary sequences, well-constrained chronologies, and good stratigraphic resolution, thus confirming that buried archaeological remains do indeed occur in open-air sites in northwestern Patagonia.

The sedimentary context of archaeological materials at APE-8B, APE-14, CAR-1, and MR-6 was formed by eolian and mixed fluvial-eolian processes, associated with ephemeral streams under sedimentological and geomorphological conditions similar to the arid to semiarid conditions of today. Eolian sedimentation is mainly associ-

ated with eolian sand sheets that include coppice dunes, sand shadows, and partially vegetated, unrippled mantles. These eolian sediments have been subject to reworking by low-energy fluvial currents and sandy gravity flows. The nature of this stratigraphy documents intertwined alluvial and eolian processes within a dryland landscape, a depositional system described as fluvial-eolian interaction (Bullard & Livingstone, 2002; Langford, 1989; Tripaldi & Limarino, 2008).

Post-depositional processes, including bioturbation, pedogenesis, and/or human activity, work to obliterate the depositional sedimentary structures resulting in massive deposits that lack internal bedforms. In our study sites, some degree of post-depositional modification cannot be ruled out. However, there is little evidence of these processes, leading us to conclude that the lack of internal bedding in many of the deposits is original and related to depositional processes associated with eolian sand sheets and fluvial-eolian environments that tend not to produce internal bedding (e.g., Forman et al., 2014; Lea, 1990; Tripaldi & Limarino, 2008).

The four excavated sites illustrate different geoarchaeological processes and depositional histories, marked by variable eolian and fluvial influence that led to the burial and preservation of the archaeological materials (Fig. 12). All of the study localities are located in dryland alluvial plain settings but show different sedimentary trends due to shifts in fluvial versus eolian morphogenesis, a typical feature of dynamic fluvial-eolian systems (Langford, 1989). In this sense, there are two extremes of the depositional process with inverted successions, likely linked to localized geomorphic differences. The MR-6 and CAR-1 sedimentary successions are distinctly bedded, in comparison

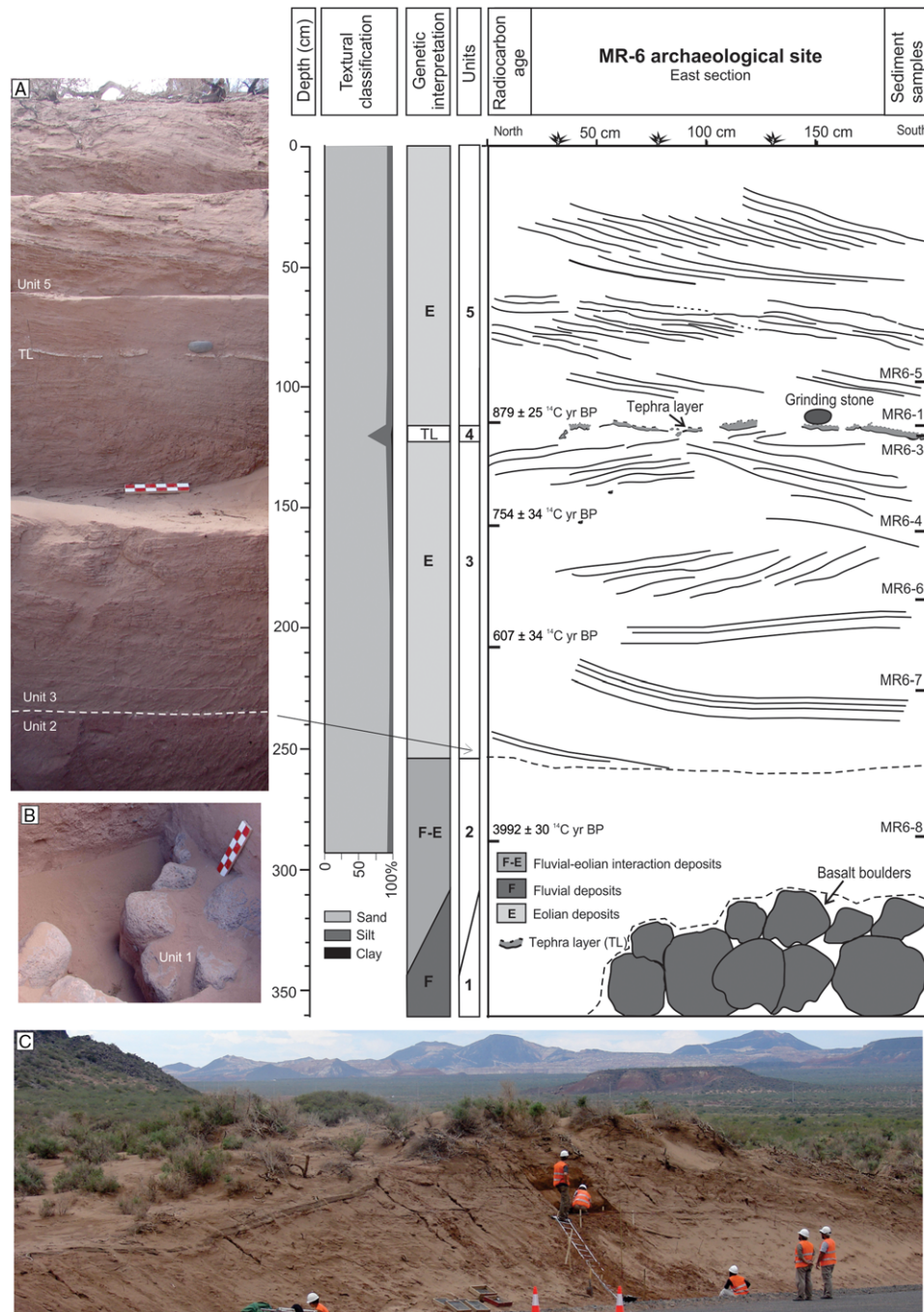


**FIGURE 10** Stratigraphy at MR-6 (Colorado Valley locality), with particle size, sample location,  $^{14}\text{C}$  ages, sediment units and their genetic interpretations. Field pictures include (A) cross-bedded eolian sand (Units 3 and 5) overlying a massive fluvial-eolian deposit (Unit 2) and showing a white tephra layer (Unit 4) with a grinding stone above it, (B) basalt boulders (Unit 1) at the base of the archaeological excavation, and (C) location of the MR-6 site excavations into a coppice dune [Color figure can be viewed at [wileyonlinelibrary.com](http://wileyonlinelibrary.com)]

to the APE-8B record that contains a more homogenous stratigraphy (Fig. 12). At MR-6 the stratigraphy is characterized by initial alluvial deposition that gradually changes to combined fluvial-eolian sedimentation and ends with eolian deposition. In contrast, the CAR-1 depositional sequence begins with eolian deposition and is followed by a fluvial-eolian sedimentation. The relatively homogenous APE-8B deposit formed mostly by fluvial-eolian sedimentation, with punctuated fluvial events (Fig. 12).

## 6.2 | Archaeological resolution

Human occupation at sites APE-8B and MR-6 were discrete and discontinuous, spatially and temporally, resulting in stratigraphic separation and high chronological resolution (Fig. 12). This is fortuitous given that cultural deposits in eolian dunes, and sometimes in fluvial terraces are commonly found in a continuous and mixed manner (Waters, 1992: 195), such as at CAR-1 (Fig. 12). Cultural material in the fluvial-eolian deposits at CAR-1 is continuous over a significant depth and very

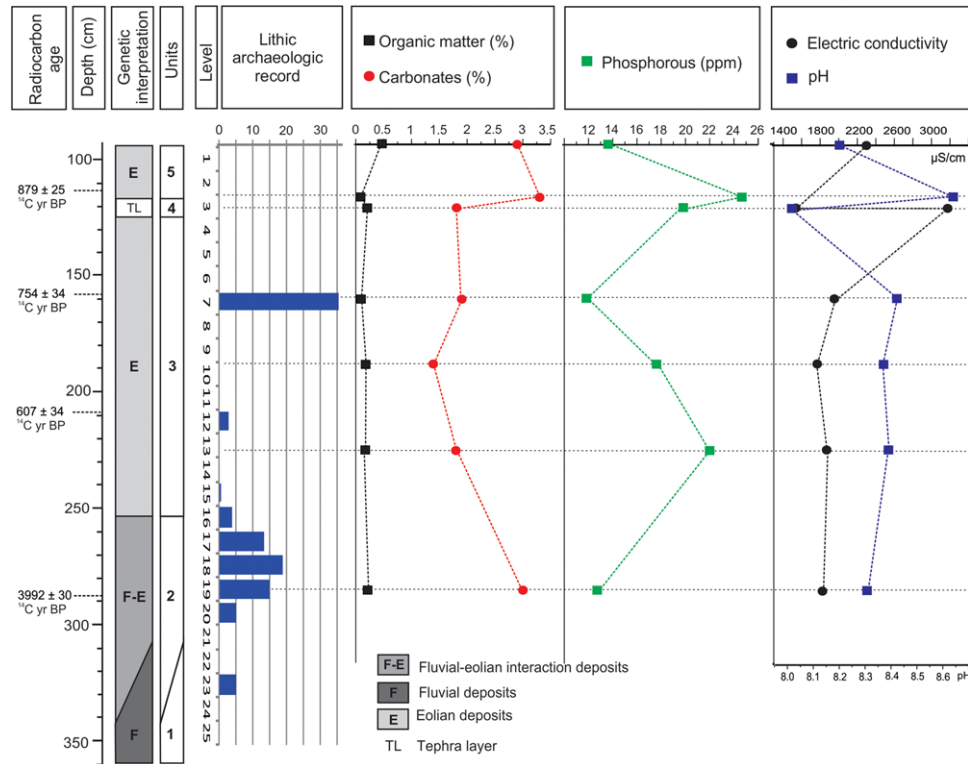


**FIGURE 11** Archaeological lithic material and chemical parameters in relation to sediment units and their genetic interpretations at MR-6 (Colorado Valley locality) [Color figure can be viewed at [wileyonlinelibrary.com](http://wileyonlinelibrary.com)]

dense, suggesting disturbance by post-depositional processes. Lower artifact density in the lower deposits (Unit 1) at CAR-1 is probably related to higher eolian sedimentation rates.

Archaeological excavations presented here provide the earliest evidence yet for human occupation within the southern margin of Payunia in northwestern Patagonia with cultural materials dating as early as  $\sim 7300$   $^{14}\text{C}$  yr B.P. at APE-14 and  $\sim 5700$   $^{14}\text{C}$  yr B.P. at APE-14 and CAR-1 (Figs 7 and 8). The low density of artifacts suggests short-term human occupations associated with foraging. Younger archaeological remains document human activity in the area between  $\sim 600$ – $900$   $^{14}\text{C}$  yr B.P. at MR-6 and  $\sim 610$ – $370$   $^{14}\text{C}$  yr B.P. at APE-8B (Figs 3 and 10). Archaeological materials recovered in Unit 5 at CAR-1 suggests that the Carmonina locality was a base camp, with strong evidence of lithic tool manufacturing and plant processing (indicated by several hand and milling stones). Despite deposits that hinder bone preservation, bone remains and *Rhea* egg shell fragment imply that animal resources were processed at this site. The proximity of CAR-1 to a freshwater spring, presumably present during human occupation, favored the concentration of human activity in the same place resulting in a higher rate of artifact deposition, limited stratigraphic separation, and low temporal resolution. Overall, the archaeological evidence supports human occupation by highly mobile hunter-gatherers groups.

In contrast to CAR-1, the APE-8B site presents discrete, stratigraphically separated cultural deposits with high temporal resolution reflective of repeated, short human occupation events. In addition, numerous archaeological remains recording short and discrete occupation events commonly occur some distance along the steep-sided walls of the Agua de Pérez arroyo. The nature of this setting, with an

extended terrace adjacent to a small and partially entrenched channel, likely favored a more spatially extensive human occupation at the site. Even when the place was frequently reoccupied, these occupations rarely occurred at the same place resulting in a more discontinuous and dispersed archaeological record well preserved by rapid fluvial-eolian sedimentary processes.

The archaeological record at MR-6 corresponds to a short-term, probably restricted activity site that reflects a relatively homogeneous landscape dominated by the Colorado River and associated fluvial-eolian plains, similar to the APE-8B and APE-14 sites. The area contains several coppice dunes similar to that excavated at MR-6 that are likely to contain subsurface cultural deposits over a broad area.

## 7 | CONCLUSION

The geoarchaeological approach followed in our study of four sites in the Cañadón Amarillo area of northwestern Patagonia emphasized the sedimentological and geomorphological context of cultural remains. Our results indicate that interchannel areas of ephemeral streams may contain relatively intact subsurface archaeological materials within deposits formed by fluvial-eolian interactions. In terms of human activity, the ephemeral streams provided water and food resources in an open setting conducive for dispersed, episodic occupations. At the four sites, depositional processes dominated by eolian and low-energy fluvial activity helped to quickly bury archaeological materials, protecting them from erosion and helping to preserve spatially



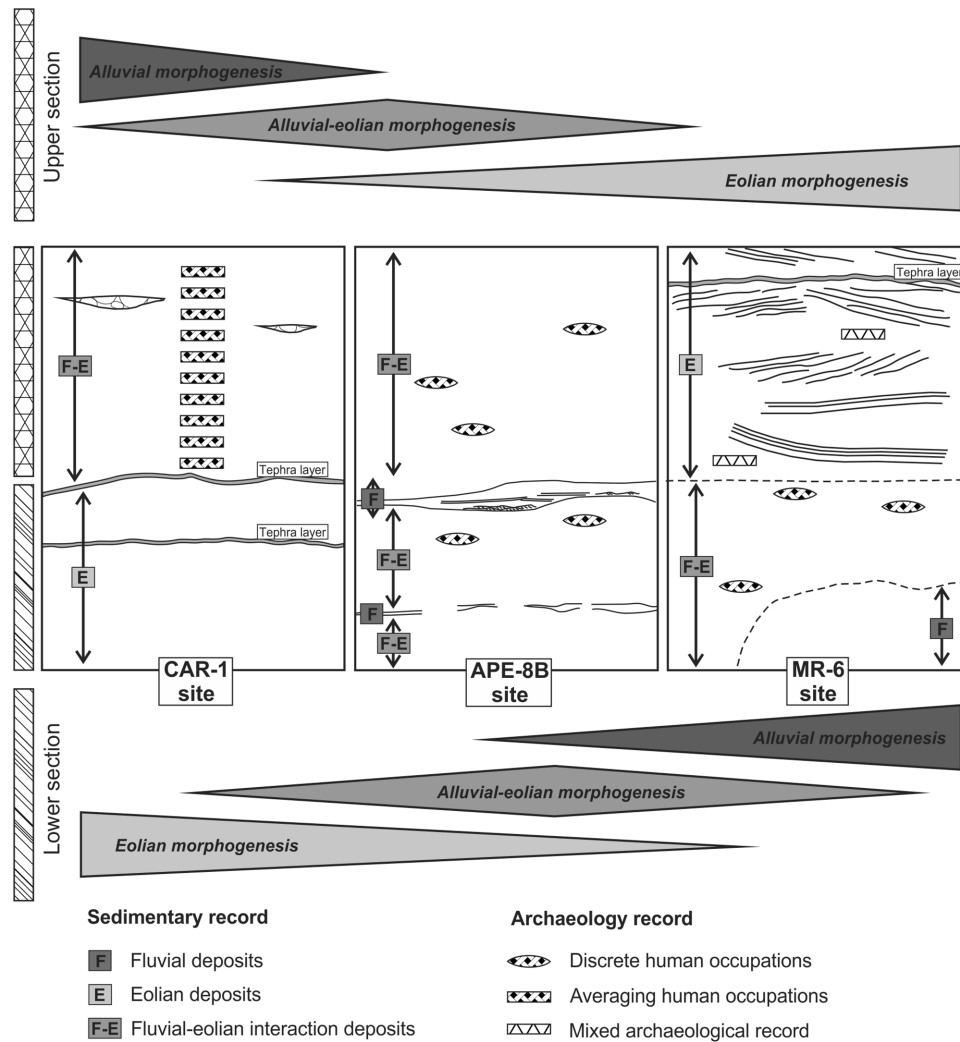


**FIGURE 12** Geoarchaeological scheme of site formation at APE-8B, MR-6, and CAR-1 (not to scale) showing the variable influence of natural depositional processes (fluvial and eolian morphogenesis) on sediment accumulation (eolian, fluvial, and fluvial-eolian deposits) and its relation to the occurrence of archaeological remains

and temporally discrete archaeological layers. Radiocarbon dating of these layers indicate human occupation as early as  $\sim 7300$   $^{14}\text{C}$  yr B.P., the oldest cultural evidence thus far identified for the Payunia and Cañadón Amarillo area.

The archaeological record within the study area displays variable stratigraphic and temporal resolution ranging from high at APE-8B, APE-14, and MR-6 to relatively low at CAR-1. This variability is likely related to depositional processes and the geomorphic setting of the archaeological sites. In this regard, material evidence of human occupations in fluvial-eolian contexts exhibit better integrity and resolution than archaeological sites solely in eolian dune deposits. Detailed geoarchaeological analysis of natural stratigraphic exposures in stream-cuts combined with archaeological surface exploration demonstrated numerous buried open-air sites in the Cañadón Amarillo area. These sites significantly expand our knowledge of human prehistory in the area. Future geoarchaeological research in this area will continue to play an important role in obtaining a more complete panorama of past human dynamics in the dryland settings of southern South America.

## ACKNOWLEDGMENTS

This work was supported by the Universidad de Buenos Aires (UBACyT 20620100100009 and UBACyT20620130100002BA), the CONICET (PIP 5819), and the ANPCyT (PICT 2012-1512 and 2012-0881). The collaboration in the field of our colleagues and the assistance at the field and laboratory analysis by the Vale-Potasio Río Colorado Company is highly appreciated. We thank the Co-Editors and the anonymous reviewers for their constructive comments, which helped us to improve the manuscript.

## REFERENCES

- Barberena, R. (2014). Discordancias y discontinuidades en Patagonia septentrional: Crono-estratigrafía de Cueva Huenul 1 (Neuquén, Argentina). In V. Cortegoso, V. Durán, & A. Gasco (Eds.), *Arqueología de ambientes de altura en Mendoza y San Juan* (203–219). Mendoza: EDI-UNC, Universidad Nacional de Cuyo.
- Barberena, R. (2015). Cueva Huenul 1 archaeological site (Northwestern Patagonia, Argentina): Initial colonization and mid-Holocene demographic retraction. *Latin American Antiquity*, 26(3)304–318.

- Barberena, R., Hajduk, A., Gil, A. F., Neme, G. A., Durán, V., Glascock, M. D., ... Rughini, A. (2011). Obsidian in the south-central Andes: Geological, geochemical, and archaeological assessment of north Patagonian sources (Argentina). *Quaternary International*, 245, 25–36.
- Barberena, R., Pompei, M. P., Otaola, C., Gil, A. F., Neme, G. A., Borrazzo, K., ... Huguin, R. (2010). Pleistocene-Holocene transition in Northern Patagonia: Evidences from Huenul cave (Neuquén, Argentina). *Current Research in the Pleistocene*, 27, 5–8.
- Bazzanella, M., & Wierer, U. (2013). Shelters Mandra di Dos Capel and Trato and the Beginning of Pastoralism in Fiemme Valley, Trentino (Italy). In F. Lugli, A.A. Stoppiello, & S. Biagetti (Eds.), *Ethnoarchaeology: Current Research and Field Methods* (181–186). Conference Proceedings Rome, Italy 13th–14th May 2010, in BAR International Series 2472 Oxford: Archaeopress.
- Berón, M. A. (2007). Integración de evidencias para evaluar dinámica y circulación de poblaciones en las fronteras del río Colorado. In F. Morello, A. Prieto, M. Martinic, & G. Bahamonde (Eds.), *Arqueología de Fuego-Patagonia. Levantando piedras, desenterrando huesos y develando arcanos* (173–188). Punta Arenas: CEQUA.
- Boggs, S. Jr. (2006). *Principles of sedimentology and stratigraphy* (4th ed., 662). New York: Pearson Prentice Hall.
- Borrero, L. A. (1989). Evolución cultural divergente en la Patagonia austral. *Anales del Instituto de la Patagonia. Serie Ciencias Sociales*, 19, 133–140.
- Borrero, L. A. (2004). The archaeozoology of Andean “dead end” in Patagonia: Living near the continental ice cap. In M. Mondini, S. Muñoz, & S. Wickler (Eds.), *Colonization, migration, and marginal areas. A zooarchaeological approach* (pp55–61). Oxford: Oxbow Books.
- Bray, R. M., & Kurtz, L. T. (1945). Determination of total, organic, and available forms of phosphorus in soils. *Soil Science*, 59, 39–45.
- Bronk Ramsey, C., Scott, E. M., & van der Plicht, J. (2013). Calibration for archaeological and environmental terrestrial samples in the time range 26–50 Ka Cal B.P., *Radiocarbon*, 55(4), 2021–2027.
- Bruniard, E. (1982). La diagonal árida Argentina: Un límite climático real. *Revista Geográfica*, 95, 5–20.
- Buck, F. J., Kipp, J. Jr., & Monger, H. C. (2002). Inverted clast stratigraphy in an eolian archaeological environment. *Geoarchaeology*, 17, 665–687.
- Bull, W. B. (1997). Discontinuous ephemeral streams. *Geomorphology*, 19, 227–276.
- Bullard, J. E., & Livingstone, I. (2002). Interactions between aeolian and fluvial systems in dryland environments. *Area*, 34, 8–16.
- Corbat, M. (2016). Variabilidad ambiental y sociocultural en la explotación de peces en el centro-occidente argentino: Una evaluación zooarqueológica (Unpublished PhD Thesis). Universidad de Buenos Aires, Buenos Aires, Argentina.
- Dincauze, D. F. (2000). *Environmental archaeology: principles and practice*. Cambridge: Cambridge University Press.
- Durán, V. (2000). *Poblaciones Indígenas de Malargüe. CEIDER, Serie libros N° 1. Facultad de Filosofía y Letras*. Mendoza: Universidad Nacional de Cuyo.
- Durán, V., & Mikkan, R. (2009). Impacto del volcanismo holocénico sobre el poblamiento humano del sur de Mendoza (Argentina). *Intersecciones en Antropología*, 10, 295–310.
- Ferrer, J.A., & Regairaz, M.C. (1993). Suelos de Mendoza: factores y procesos de formación. *XII Congreso Geológico Argentino* (633–642). Mendoza: Relatorio de la Provincia de Mendoza.
- Fernández, J. (1988–1990). La cueva de Haichol. Arqueología de los pinares cordilleranos del Neuquén. *Anales de Arqueología y Etnología*, 43–45.
- Folk, R. L., Andrews, P. B., & Lewis, D. W. (1970). Detrital sedimentary rock classification and nomenclature for use in New Zeland. *New Zeland Journal of Geology and Geophysics*, 13, 937–968.
- Folk, R. L., & Ward, W. C. (1957). Brazos River bar – A study in the significance of grain-size parameters. *Journal of Sedimentary Petrology*, 27(1), 3–27.
- Forasiepi, A., Martinelli, A., Gil, A. F., Neme, G. A., & Cerdeño, E. (2010). Fauna extinta y ocupaciones humanas en el Pleistoceno final-Holoceno temprano del centro occidental argentino. In M. Gutiérrez, M. De Nigris, P. M. Fernández, M. Giardina, A. F. Gil, A. Izeta, ... H. D. Yacobaccio (Eds.), *Zooarqueología a principios del Siglo XXI: Aportes teóricos, metodológicos y casos de estudio* (219–229). Buenos Aires: Ediciones El Espinillo.
- Forman, S. L., Tripaldi, A., & Ciccioli, P. L. (2014). Eolian sand sheet deposition in the San Luis paleodune field, western Argentina as an indicator of a semi-arid environment through the Holocene. *Palaeogeography, Palaeoclimatology and Palaeoecology*, 411, 122–135.
- García, A. (2010). Human occupation during the mid-Holocene in western Argentina: A comment on Neme and Gil. *Current Anthropology*, 51, 415–416.
- Garreaud, R., Vuille, M., Compagnucci, R., & Marengo, J. (2009). Present-day South American Climate. *PALAEO3 Special Issue (LOTRED South America)*, 281, 180–195.
- Gil, A. F. (2006). *Arqueología de La Payunia (Mendoza, Argentina). El poblamiento humano en los márgenes de la agricultura. Bar International Series 1477*. Oxford.
- Gil, A. F., & Neme, G. A. (2006). Distribuciones arqueológicas superficiales en Payunia-Llancanelo. *Anales de Arqueología y Etnología*, 61, 163–184.
- Goñi, R. (1995). Aleros: Uso actual e implicancias arqueológicas. *Cuadernos Instituto Nacional Antropología y Pensamiento Latinoamericano*, 16, 329–342.
- Gorecki, P. (1988). Hunters and shelters—The need for ethnoarchaeological data. In B. Meehan & R. Jones (Eds.), *Archaeology with ethnography: An Australian perspective* (159–170). Canberra: Australian National University, Research School of Pacific Studies.
- Gorecki, P. (1991). Horticulturalists as hunter-gatherers: Rockshelter usage in Papua New Guinea. In C. S. Gamble & W. A. Boismier (Eds.), *Ethnoarchaeological approaches to mobile campsites* (pp. 237–262). Ethnoarchaeological Series 1, Ann Arbor: International Monographs in Prehistory.
- Gradín, C. J. (1984). *Investigaciones arqueológicas en Casa de Piedra. Pcias. de Buenos Aires, La Pampa y Río Negro*. Santa Rosa: Ente Ejecutivo Casa de Piedra, Ministerio de Educación y Cultura de la provincia de La Pampa.
- Hogg, A. G., Hua, Q., Blackwell, P. G., Niu, M., Buck, C. E., Guilderson, T. P., ... Zimmerman, S. R. H. (2013). SHCal13 Southern Hemisphere calibration, 0–50,000 years cal BP. *Radiocarbon*, 55(4), 1889–1903.
- Lagiglia, H. (1977). Dinámica Cultural del Centro Oeste y Sus Relaciones con Áreas Aledañas Argentinas y Chilenas. *Actas del VII Congreso Nacional de Arqueología Chilena*. Vol. 2, Sociedad Chilena de Arqueología. Altos de Vilches, 532–560.
- Lagiglia, H. (1980). El precerámico final en el sur de Cuyo. *Actas del V congreso nacional de arqueología Argentina*, Tomo I, Instituto de Investigaciones Arqueológicas y Museo, Universidad Nacional de San Juan. San Juan, 55–60.
- Langford, R. P. (1989). Fluvial-aeolian interactions: Part I, modern systems. *Sedimentology*, 36, 1023–1035.
- Lea, R. D. (1990). Pleistocene periglacial eolian deposits in southwestern Alaska: Sedimentary facies and depositional processes. *Journal of Sedimentary Petrology*, 60, 582–591.
- Llambías, E. J., Bertotto, G. W., Risso, C., & Hernando, I. R. (2010). El volcanismo cuaternario en el retroarco de Payenia: Una revisión. *Revista de la Asociación Geológica Argentina*, 67(2), 278–300.
- Martínez Carretero, E. (2004). La Provincia Fitogeográfica de la Payunia. *Boletín Sociedad Argentina de Botánica*, 39(3–4), 195–226.

- Miall, A. D. (1996). *The geology of fluvial deposits* (p. 582). Berlín: Springer Verlag.
- Munsell Color, (2000). *Munsell Soil Color Chart*. Kollmorgen, Baltimore: Macbeth Division.
- Narciso, V., Santamaría, G., Zanettini, J. C. M., & Leanza, H. A. (2004). *Hoja Geológica 3769-I "Barrancas", provincias de Mendoza y Neuquén, escala 1:250.000* (6). Buenos Aires: SEGEMAR.
- Neme, G. A., & Gil, A. F. (2009). Human occupation and increasing Mid-Holocene Aridity: Southern Andean Perspectives. *Current Anthropology*, 50(1), 149–163.
- Neme, G. A., & Gil, A. F. (2012). El registro arqueológico del sur de Mendoza en perspectiva biogeográfica. In G. A. Neme & A. F. Gil (Eds.), *Paleoecología Humana en el sur de Mendoza: Perspectivas Arqueológicas*, (255–279). Buenos Aires: Sociedad Argentina de Antropología.
- Neme, G. A., Gil, A. F., Garvey, R., Llano, C. L., Zangrando, A. F., Francheti, F., ... Michieli, C. T. (2011). El registro arqueológico de la Gruta de El Manzano y sus implicancias para la arqueología de Nordpatagonia. *Magallania*, 9, 243–265.
- Newell, A. J. (2001). Bounding surfaces in a mixed aeolian–fluvial system (Rotlegend, Wessex Basin, SW UK). *Marine and Petroleum Geology*, 18, 339–347.
- Ramos, V. A., & Folguera, A. (2010). Payenia volcanic province in the Southern Andes: An appraisal of an exceptional Quaternary tectonic setting. *Journal of Volcanology and Geothermal Research*, 201(1–4), 53–64.
- Reading, H. G. (1996). *Sedimentary environments and facies* (3rd ed., 688). Oxford: Blackwell Scientific Publications.
- Salgán, L. (2012). *Organización tecnológica y biogeografía humana en La Payunia, sur de la provincia de Mendoza* (Unpublished PhD Thesis). Universidad Nacional de La Plata, La Plata.
- Salgán, L., Gil, A. F., & Neme, G. A. (2012). Obsidianas en la Payunia (sur de Mendoza, Argentina): Patrones de distribución e implicancias en la ocupación regional. *Magallania*, 40, 263–277.
- Schiffer, M. B. (1996). Some relationship between behavioral and evolutionary archaeologies. *American Antiquity*, 61, 643–662.
- Servicio Meteorológico Nacional. (1992). *Estadísticas Climatológicas N° 37. 1981–1990*. Buenos Aires: Servicio Meteorológico Nacional.
- Stein, J. K., & Farrand, W. R. (Eds.). (2001). *Sediments in archaeological context*. Salt Lake City: University of Utah Press.
- Stern, C. R. (2004). Active Andean volcanism: Its geologic and tectonic setting. *Revista Geológica de Chile*, 31, 161–206.
- Tripaldi, A., & Limarino, C. O. (2008). Ambientes de interacción eólica-fluvial en valles intermontanos: Ejemplos actuales y antiguos. *Latin American Journal of Sedimentology and Basin Analysis*, 15(1), 43–66.
- Tripaldi, A., Zárate, M. A., Neme, G. A., & Gil, A. F. (2015). Paleoambientes, registro arqueológico y procesos de formación de sitios en el sur de la Payunia, provincia de Mendoza, Argentina. *VI Congreso Argentino de Cuaternario y Geomorfología*. Ushuaia: Actas, 85–86.
- Walkley, A. I., & Black, A. (1934). An examination of Degtjareff method for determining soil organic matter and a proposed modification of the chromic acid titration method. *Soil Science*, 37, 29–37.
- Waters, M. R. (1992). *Principles of geoarchaeology: A North American perspective* (401). Tucson: The Arizona University Press.

**How to cite this article:** Tripaldi A, Zárate MA, Neme GA, Gil AF, Giardina M, Salgán ML. Archaeological site formation processes in northwestern Patagonia, Mendoza Province, Argentina. *Geoarchaeology*. 2017;00:1–17. <https://doi.org/10.1002/gea.21632>